Computer study of boron and phosphorus at the Si(100)−2 × 1 surface

V.G. Zavodinsky[a], I.A. Kuyanov, and E.N. Chukurov

Institute for Automation, Far Eastern Branch of the Russian Academy of Sciences, 5 Radio, 690041, Vladivostok, Russia

Abstract. The AM1 semiempirical numerical method combined with the geometry optimization procedure was used to study the energetics of active impurities (B, P) in substitutional positions at the Si(100)–2 × 1 surface. It has been found that phosphorus prefers to be in the first layer (in dimers). Boron has the lowest energy in the second layer. Energy profits, counting from the fourth bulk-like layer, for B and P are 1.33 eV and 0.56 eV, respectively. Comparing of the P-Si and P-P dimers energetics has shown that P-Si dimers are more preferable energetically.

PACS. 82.20.Wt Computational modeling; simulation

1 Introduction

Dopant segregation near surfaces and interfaces of semiconductors is frequently investigated because of its fundamental and technological interest. According to the classical McLean model [1] the segregation process is controlled by the value of the segregation free energy which is the difference of free energies for the dopant being at the surface and in the bulk.

It is well-known that boron exhibits a temperature dependent segregation at Si surfaces [2–4]. Boron induces several kinds of Si(100) surface reconstructions (2 × 1, 2 × 2, 4 × 4) differentiated by B concentrations and atomic geometries [5–7]. In all these surface phases boron has a tendency to be in subsurface layers, substituting bulk Si atoms. As for phosphorus, it does not induce any new reconstruction on the Si(100)-2 × 1 surface [8]. However, Hamers *et al.* [9,10] using scanning tunneling microscopy, observed P-P and Si-P dimers on this surface. Thus the behaviours of boron and phosphorus at the Si(100)–2 × 1 surface are quite different.

The present work is a computational attempt to obtain some quantitative information on the energetics of B and P on the Si(100)–2 × 1 surface and in subsurface layers.

2 Method of calculations and its verification

To calculate the total energy of silicon-dopant systems we used the advanced semiempirical quantum-chemical method AM1 (Austin Model 1) [11], a version of the Modified Intermediate Neglect of Differential Overlap(MINDO) [12–14], realized in the frame of the

a e-mail: `vzadov@mailcity.com`

CLUSTER-Z1 package [15,16]. This package allows to optimize atomic configurations by the minimization of the total energy gradients over all atomic coordinates.

Semiempirical methods are significantly faster than *ab initio* methods, but their accuracy is limited by the need to choose the correct set of parameters. In particular, AM1 is usually parametrized to reproduce heats of atomization and molecular geometries. Therefore, the ability of a semiempirical method to describe an arbitrary configuration of atoms must be verified.

The AM1 method was verified for silicon-boron systems in our recent work [17] where the B/Si(111)–$(\sqrt{3} \times \sqrt{3})$ system was studied comparing energies of the B-T_4, B-H_3 and B-S_5 cases. It has been found that the B-S_5 case has the lowest binding energy per a B atom. Its absolutely value is ≈ 6 eV, and the B-T_4 and B-H_3 values are higher by 1.1 eV and 2.2 eV, respectively. These differences (ΔE) are in excellent agreement with the *ab initio* calculations of Kaxiras *et al.* [18] ($\Delta E_{T_4} = 1$ eV, $\Delta E_{H_3} = 2.1$ eV) and Bedrossian *et al.* [19] ($\Delta E_{T_4} = 0.93$ eV).

3 Results and discussions

3.1 Single B and P atoms

For our calculations we used the $Si_{83}H_{64}$ cluster shown in Figure 1a. This cluster consists of 83 Si atoms modeling the Si(100)–2 × 1 surface with six atomic layers where broken Si bonds are saturated with 64 H atoms. Initially all Si atoms were placed in ideal bulk positions and all Si-H distances were equal to equilibrium 1.46 Å values. During the optimization procedure all H atoms were fixed.

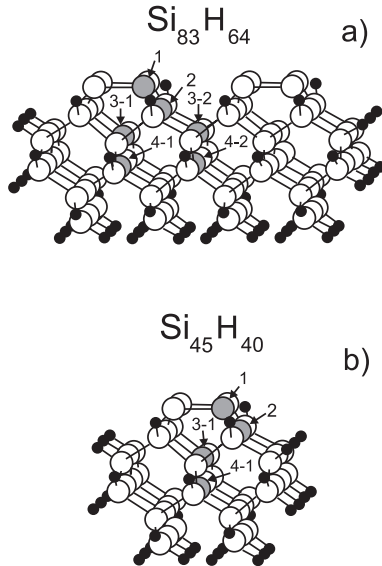Without dopants, the stable Si(100)–2 × 1 geometry was determined. Like the known cluster investigations

Fig. 1. Atomic schemes of the $Si_{83}H_{64}$ (a) and $Si_{45}H_{40}$ (b) clusters modeling the Si(100)–2 × 1 surface. White circles are Si atoms; black circles are H atoms. Si atoms substituted by dopants are shown as grey circles. They are marked by arrowed numbers as it is described in the text.

Table 1. Energetics of B and P substitutional single atoms at the Si(100)–2 × 1 surface and in subsurface layers. Energies are given with respect to the fourth layer (4-1 site).

Layer (site)	$Si_{83}H_{64}$ B	P	$Si_{45}H_{40}$ B	P
1	−1.11	−0.56	−1.30	−0.39
2	−1.43	0.55	−1.41	0.22
3 (3-1)	−0.35	−0.27	−0.33	−0.10
3 (3-2)	0.18	−0.14		
4 (4-1)	0	0	0	0
4 (4-2)	−0.10	0.25		

[20–22] the symmetric dimer stable structure was obtained (2 rows × 2 dimers in Fig. 1). It seems that the asymmetric dimer structure, reported by numerous authors [23–28] using zone methods, has a cooperative origin and can not be obtained in a cluster approach. The dimer length was found to be 2.15 Å for the singlet spin state and 2.40 Å for the triplet one. (Experimental value is 2.3 Å [29].) The triplet state was found to be more stable energetically ($E_{tripl} - E_{singl} = -3.76$ eV), thus this state was used for the following calculations.

Then we placed B and P single atoms in substitutional positions in the first, second, third and fourth layers as it is marked in Figure 1. As it is clear from Figure 1a there are nonequivalent sites in the third and fourth layers of the studied cluster. We marked them as 3-1, 3-2, 4-1, 4-2 and studied them specially. The 3-1 and 4-1 sites are situated directly under a dimer row, while the 3-2 and 4-2 sites lie between the dimer rows.

In order to study the size effect we have carried out similar calculations using a small cluster ($Si_{45}H_{40}$) shown

in Figure 1b. This cluster consists of 45 Si atoms and has two surface Si dimers.

Results of calculations are summarized in Table 1. The main result is that the energetics of boron and phosphorus near the Si(100)–2 × 1 surface are rather different. Boron has a possibility to substitute Si atoms in dimers, however the most favour position is a substitution site in the second atomic layer where the bulk-like surrounding is present. This fact agrees with the model of the formation of the boron-induced phases at the Si(100) surface [9,18], in which boron atoms substitute into the first full atomic layer of the Si lattice. This layer is then capped with Si-Si dimers and/or dimer vacancies. The relative numbers of Si-Si dimers and dimer vacancies can vary, resulting in several related reconstructions.

Energetics of phosphorus does not permit a P atom to be in the second atomic layer (the energy difference is positive). At the other hand phosphorus can substitute silicon in the first layer and can form Si-P dimers in accordance with experiments [9,10].

Table 1 demonstrates some dependence of results on a cluster size. However one can see that the size dependence is not principal and does not change above conclusions. It is doubtful that results obtained with larger clusters would be drastically different from present ones.

3.2 P-Si and P-P dimers

The formation of P-Si and P-P dimers was investigated by Hamers *et al.* [9,10] using scanning tunneling microscopy. Counting statistics were used to study the equilibrium between Si-Si, P-Si, and P-P dimers, showing that the formation of P-Si heterodimers is more preferable. *Ab initio* molecular orbital calculations [9] have shown that the overall energy change for 2Si-P → Si-Si + P-P is +0.27 eV, or about +0.13 eV per P-Si dimer. Each dimer (Si-Si, P-P or P-Si) was studied using a separate Si_9H_{12} cluster (Fig. 2a) modeling the Si(100) surface (only 1 surface dimer, all H atoms are fixed); then energies of two clusters [(P-Si) + (P-Si) or (P-P) + (Si-Si)] were summarized and the difference [(P-Si) + (P-Si)] - [(P-P) + (Si-Si)] was calculated. In other words, the correlation between dimers was ignored and a small cluster approach was used.

We have here a possibility to study correlated dimers and to use large clusters. First of all we have carried out the calibrate calculations using the same cluster and the same methodics as it was used in [9]. The energy profit for (P-Si)+(P-Si) → (Si-Si) + (P-P) was found to be 0.35 eV, or about 0.18 eV per P-Si dimer. The agreement with *ab initio* results of Hamers, Wang and Shan [9] is rather good. To study the cluster size effect for noncorrelated dimers we repeated the above calculations using larger clusters ($Si_{19}H_{28}$, $Si_{22}H_{32}$ with 2 dimers and $Si_{35}H_{44}$ with 4 dimers) shown in Figures 2b to 2d. These clusters had three atomic layers (one dimerized and two bulk). Likely the small cluster case, only one of the dimers may be a P-P or P-Si dimer. The (P-P) + (Si-Si) or (P-Si) + (P-Si) energies were obtained as summs of energies of corresponding
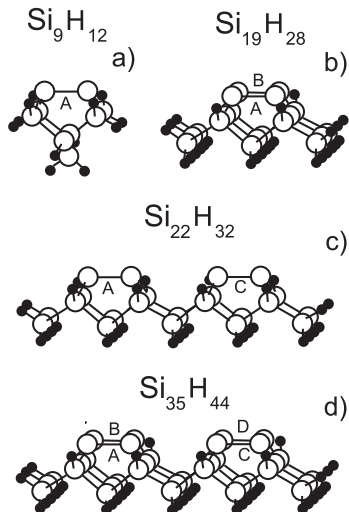
Fig. 2. Clusters used to compare the energetis of P-Si and P-P dimers. White circles are Si atoms; black circles are H atoms. Letters A, B, C, and D are used for marking the different dimers as it is cleared in the text.

Table 2. Energy differences of the (P-Si) + (P-Si) and (P-P) + (Si-Si) noncorrelated dimer systems at the Si(100)-2×1 surface. Each dimer is on a separate cluster. The Si_9H_{12} cluster has one surface dimer; the $Si_{19}H_{28}$ cluster has one row with two dimers; the $Si_{22}H_{32}$ cluster has two dimers in neighbouring rows; the $Si_{35}H_{44}$ cluster has two rows with two dimers in each.

Si_9H_{12}		$Si_{19}H_{28}$	$Si_{22}H_{32}$	$Si_{35}H_{44}$
Hamers [9]	Present			
0.27	0.35	1.09	1.11	0.82

clusters. All results for noncorellated dimers are collected in Table 2.

The correlation between P-Si dimers was studied placing two P-Si dimers at the same cluster (one of the $Si_{19}H_{28}$, $Si_{22}H_{32}$, $Si_{35}H_{44}$ clusters shown in Fig. 2). Because P-Si dimers may be oriented by different ways we studied the following different cases:

1) AB/PSi-PSi. Two P-Si dimers with identical orientations in the same row.

2) AB/PSi-SiP. Two P-Si dimers with opposite orientations in the same row.

3) AC/PSi-PSi. Two P-Si adjacent dimers with identical orientations in different rows.

4) AC/PSi-SiP. Two P-Si adjacent dimers with opposite orientations in different rows. Si atoms look out at the same valley.

5) AC/SiP-PSi. Two P-Si adjacent dimers with opposite orientations in different rows. Si atoms look out at different valleys.

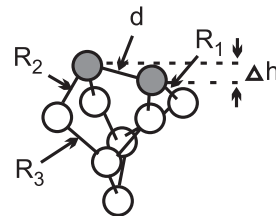6) AD/PSi-PSi. Two P-Si nonadjacent dimers with identical orientations in different rows.

Fig. 3. Generalized atomic scheme of Si-Si, P-Si, and P-P dimers. Grey cirles represent Si atoms which may be substituted by P. d is the dimer length; Δh is the height difference of dimer atoms; R_1 and R_2 are the bond lengths between dimerized atoms and the underlaying Si layer; R_3 is the bond length between Si atoms of first and second bulk layers. In the P-Si case, the lowest dimer atom is the P atom.

7) AD/PSi-SiP. Two P-Si nonadjacent dimers with oppozite orientations in different rows. Si atoms look out at the same valley.

8) AD/SiP-PSi. Two P-Si nonadjacent dimers with oppozite orientations in different rows. Si atoms look out at different valleys.

Letters A, B, C, and D are used for marking the different dimers (see Fig. 2). For example, AC/SiP-PSi means that this case includes a A/SiP dimer in the one row and a C/PSi dimer in the second row. Orientations of the dimers are opposite. Results for correlated dimers are summarised in Table 3.

Analysing data of Tables 2 and 3 one can see that the size effect for the noncorrelation approach is rather large. The energy difference for the(P-Si)+(P-Si) → (Si-Si) + (P-P) transition changes from 0.35 eV to 0.82 eV as moving from Si_9H_{12} to $Si_{35}H_{44}$. The 0.82 eV value, obtained for the largest ($Si_{35}H_{44}$) cluster without taking into account the P-Si–P-Si correlations, is very close to the values (0.82 eV–0.86 eV) obtained for the P-Si–P-Si correlated pairs situated in different dimer rows at the same cluster. In the other words, speaking, the correlation of P-Si dimers, which are situated in different rows, is very small. At the other hand, energy of a P-Si–P-Si pair, which is situated in the same row, depends on the mutual orientation of P-Si dimers: Energy is lower for P-Si dimers with the same orientation. For cases in which dimers are in different rows the mutual dimer orientation is practically negligible. Small increasing of energy up to 1.09–1.11 eV for the middle clusters ($Si_{19}H_{28}$ and $Si_{22}H_{32}$) may be the result of the known size oscillation effect.

It is interesting to compare our Si-Si, P-Si and P-P dimer geometries with the data obtained by Wang, Chen and Hamers [10]. The generalized atomic scheme of the dimers is shown in Figure 3. Calculated geometry parameters are collected in Table 4. One can see that the discrepancy between our results and results of Wang *et al.* is rather small except the P-P dimer bond. We have found this bond much shorter (of 0.21 Å) than Wang, Chen and Hamers have published. However, it must be noted that the data presented in [10] are not the real experimental or numerical calculated data. They are the products of some chemical qualitative speculations and must not be considered as reliable quantitative results.

Table 3. Energy differences of (P-Si + P-Si) and (P-P + Si-Si) correlated dimer systems at the Si(100)-2 × 1 surface. Dimers of the studied dimer pair are situated at the same cluster. The numbers 1, 2, ..., 8 correspond to the cases described in the text.

| | Dimers in the same row | | Dimers in different rows | | | | | |
| | | | Adjacent dimers | | | Nonadjacent dimers | | |
	1	2	3	4	5	6	7	8
$Si_{19}H_{28}$	0.89	0.73						
$Si_{22}H_{32}$			0.94	0.92	0.96			
$Si_{35}H_{44}$	0.91	0.47	0.83	0.82	0.85	0.83	0.83	0.86

Table 4. Geometry parameters of Si-Si, P-Si and P-P dimers on Si(100). Details are described in the captions of Figure 3.

| | Wang *et al.* [10] | | | | | Present | | | | |
	d	Δh	R_1	R_2	R_3	d	Δh	R_1	R_2	R_3
Si-Si	2.30	–	2.41	2.41	2.35	2.42	0	2.38	2.38	2.37
P-Si	2.25	0.30	2.25	2.35	2.35	2.16	0.31	2.13	2.41	2.37
P-P	2.25	–	2.20	2.20	2.35	2.04	0	2.27	2.27	2.35

4 Conclusion

In summary, the segregation of boron and phosphorus at the Si(100)–2×1 surface may be described as a result of the moving of dopants from high-energy substituted bulk sites to low-energy surface and subsurface sites. The preferable placement for boron is the second atomic layer counting from the surface dimerized layer. Phosphorus can not substitute silicon in the second layer. It forms surface P-Si and P-P dimers, and P-Si dimers are more preferable energetically than P-P dimers.

References

1. D. McLean, *Grain Boundary in Metals* (Oxford University Press, London, 1957).
2. E. de Frésart, K.L. Wang, S.S. Rhee, Appl. Phys. Lett. **53**, 48 (1988).
3. H. Jorke, H. Kibbel, Appl. Phys. Lett. **57**, 1763 (1990).
4. M.R. Sardela Jr., W.-X. Ni, J.O. Ekberg, J.-E. Sundgren, G.V. Hansson, Mat. Res. Soc. Symp. Proc. (Materials Research Society, 1991), Vol. 220, p. 109.
5. R.L. Headrick, B.E. Weir, A.F.J. Levi, D.J. Eaglesham, L.C. Feldman, J. Cryst. Growth **111**, 838 (1991).
6. D.E. Jones, J.D. Pelz, Y. Hong, E. Bauer, I.S.T. Tsong, Phys. Rev. Lett. **77**, 330 (1996).
7. Z. Zhang, M.A. Kulakov, B. Bullemer, I. Eisele, J. Vac. Sci. Technol. B **14**, 2684 (1996).
8. V.G. Lifshits, A.A. Saranin, A.V. Zotov, *Surface Phases on Silicon: Preparation, Structures and Properties* (John Willey & Sons, Chichester, 1994).
9. R.J. Hamers, Y. Wang, J. Shan, Appl. Surf. Sci **107**, 25 (1996).
10. Y. Wang, X. Chen, R.J. Hamers, Phys. Rev. B **50**, 4534 (1994).
11. M.J.S. Dewar, E.G. Zoebisch, E.F. Healy, J.J.P. Stewart, J. Am. Chem. Soc. **107**, 3902 (1985).
12. N.C. Baird, M.J.S. Dewar, J. Chem. Phys. **50**, 1262 (1969).
13. M.J.S. Dewar, Haselbach, J. Am. Chem. Soc. **92**, 590 (1970).
14. R.C. Bingham, M.J.S. Dewar, D.H. Lo, J. Am. Chem. Soc. **97** 1285 (1975).
15. V.A. Zayetz, CLUSTER-Z1 Quantum Chemical Software (Institute of Surface Chemistry, Nat. Ac. Sci. Ukraine, Kiev, 1990).
16. V.D. Khavrytchenko, A.V. Khavrytchenko Jr., DYQUAMOD Dynamical Quantum Modeling Software for Personal Computers, (Joint Institute for Nuclear Researches, Dubna, and Institute of Surface Chemistry, Nat. Ac. Sci. Ukraine, Kiev, 1993).
17. V.G. Zavodinsky, I.A. Kuyanov, E.N. Chukurov, Phys. Low-Dim. Struct. **3/4**, 183 (1998).
18. E. Kaxiras, K.C. Pandey, F.J. Himpsel, R.M. Tromp, Phys. Rev. B **41**, 1262 (1990).
19. P. Bedrossian, R.D. Meade, K. Mortensen, D.M. Chen, J.A. Golovchenko, D. Vanderbilt, Phys. Rev Lett. **63**, 1257 (1989).
20. T. Yamaguchi, N. Fujima, Surf. Sci. **242**, 233 (1991).
21. A. Redondo, W.A. Goddard, J. Vac. Sci. Technol. **21**, 344 (1982).
22. T. Hoshino, M. Tsuda, S. Oikawa, I. Ohdomari, Surf. Sci. Lett. **291**, L763 (1993).
23. D.J. Chadi, Phys. Rev. Lett. **43**, 43 (1979).
24. M.T. Yin, M.L. Cohen, Phys. Rev. B **24**, 2303 (1981).
25. N. Roberts, R.J. Needs, Surf. Sci. **236**, 112 (1990).
26. J. Dąbrowski, M. Scheffler, Appl. Surf. Sci. **55-58**, 15 (1992).
27. A. Ramstad, G. Brocks, P.J. Kelly, Phys. Rev. B **51**, 14504 (1995).
28. R. Felici, I.K. Robinson, C. Ottaviani, P. Imperatori, P.J. Eng, P. Perfetti, Surf. Sci. **375**, 55 (1997).
29. N. Jedrecy *et al.*, Surf. Sci. **230**, 197 (1990).